Advances in Aerospace Science and Technology, 2016, 1, 21-31
Published Online June 2016 in SciRes. http://www.scirp.org/journal/aast
http://dx.doi.org/10.4236/aast.2016.11003

Journey to the Typhoon

Chung-Kiak Poh*, Chung-How Poh

Aero-Persistence Research, Penang, Malaysia
Email: *kiak@aero-persistence.com

Received 22 October 2015; accepted 2 February 2016; published 27 June 2016

Abstract

Application of UAVs (unmanned aerial vehicles) for tropical cyclone missions is an emerging area of research and recent advances include the concept of spinsonde for multi-cycle measurement of vertical wind profile within the storm. This work proposes the design of a typhoon UAV as part of a cost-effective approach for acquiring atmospheric data to improve prediction and refine models. Land- and carrier-based flight schemes are proposed in this study and computer simulations are carried out to investigate the flight performance. Results suggest that the UAV achieves a maximum cruising speed in excess of 350 km·h^{-1} with excellent spinsonde performance. Furthermore, the UAV is capable of performing high-alpha maneuvers as well as vertical landing, thus rendering it suitable for space-efficient operation whether on land or aircraft carrier.

Keywords

Tropical Cyclone, Unmanned Aerial Vehicle, Spinsonde, Vertical Wind Profile, Vertical Landing, High-Alpha Maneuvers

1. Introduction

Tropical cyclones occur worldwide and a majority of them form between a latitude of 10˚ and 30˚ away from the equator [1]. Tropical cyclones often cause widespread damage when they make landfall due to the associated high winds, torrential rainfall and storm surges [2]-[4]. A category 5 cyclone on the Saffir-Simpson Hurricane Wind Scale has a wind speed of 252 km·h^{-1} or higher [5]. Research efforts have been focused to improve the accuracy of typhoon forecast models as well as to fully understand the formation of the storm, also known as cyclogenesis [6]. Despite advances in remote sensing, *in-situ* measurements with reconnaissance flights are still necessary to obtain accurate location of pressure center and wind speeds to aid reliable forecasting [7]. The wind circulations of a matured tropical cyclone can be broadly divided into primary and secondary circulations [8]. The primary circulation refers to the tangential flow rotating about the central axis, and the secondary circulation

*Corresponding author.

How to cite this paper: Poh, C.-K. and Poh, C.-H. (2016) Journey to the Typhoon. *Advances in Aerospace Science and Technology*, **1**, 21-31. http://dx.doi.org/10.4236/aast.2016.11003

refers to the "in-up-and-out circulation" (low and middle level inflow, upper-level outflow) [8]. Thus, the general air flow model of a tropical cyclone is air parcels spiraling inwards, upwards and outwards [8]. Of particular interest to forecasters is the mean vertical wind profile (VWP) from the surface to the 700-hPa level, the altitude typically flown by reconnaissance aircraft [9]. Unmanned aerial vehicles (UAVs) have been deployed for tropical cyclone missions. Two such well-known UAVs are the NASA Global Hawk and the Aerosonde [10] [11].

Chute-operated dropsondes have been used to measure vertical wind profiles of tropical cyclones and they have a descent rate of approximately 11 ms^{-1} close to sea-level [12] [13]. They typically contain a GPS receiver, along with other sensors to record atmospheric profiles [13]. Measurement of vertical wind profile using chute-free spinsonde technique has recently been proposed, and simulations indicate that the method is promising [14]. Eliminating the bulky chute will increase payload capacity and more importantly, enable the VWP measurement to be repeated multiple time per flight [14]. Also, recent years have witnessed the advancement of radio controlled model airplanes across various classes, from sailplanes to the highly agile aerobatic airplanes. The so-called "3D aerobatic" model airplanes are well-known to be capable of performing an impressive array of post wing-stall maneuvers such as harrier (high-alpha horizontal flight), blender and torque rolls [15]. F5D is an international class ratified by the FAI (Fédération Aéronautique Internationale) which involves racing electric-powered model airplanes around a triangular course for 10 laps at speeds of approximately 322 $km \cdot h^{-1}$ [16]. All-composite airframes are commonly used in the F5D class models as they can withstand high aerodynamic stress. This allows the model airplanes to cruise and maneuver at high speed without having to resolve to morphing wing technology. The present world's speed record for model airplanes is in excess of 400 $km \cdot h^{-1}$ [17].

Given the social and economic impacts of tropical cyclones, we are endeavoring towards a cost-effective tropical cyclone research program. The overall objective is to obtain critical measurements of atmospheric data of a tropical cyclone several days prior to landfall in order to improve predictions and refine models. Desired characteristics of the typhoon UAV are high-speed cruising, spinsonde-capable, water resistance, cost-effective, and multi-agent. Pre-programmed autonomous GPS navigation will probably be used instead of a satellite-based flight control system so as to further reduce cost and complexity. The atmospheric data would be downloaded for processing and analysis once the aircraft have returned to base.

As part of the endeavor, this work presents the design of a fixed-wing typhoon UAV that incorporates the spinsonde capability and its flight performance is characterized via simulations. The target airspeed of the UAV in level flight with maximum continuous power (V_H) is 300 $km \cdot h^{-1}$ and above. The focus of this work is primarily on the airframe design and less so on the avionics. Two aircraft configurations will be evaluated in this work: 1) without drop tanks and 2) with drop tanks.

It is not uncommon for manned aircraft to penetrate the eyewalls of tropical cyclones by crabbing towards the direction of the wind to ensure radial penetrations [7] [18]. In this study however, given the nature of the flight mission, a more suitable mode of entry would be to direct the nose of the aircraft towards the eye of the storm such that the overall trajectory would be one that is spiraling inwards. In other words, the primary flow of the storm will appear as crosswind to the aircraft. The exit pattern would be similar except it would be spiraling outwards. The advantages of this approach are that the ground speeds of the aircraft into and away from the eye of storm can be regarded as independent of the intensity of the crosswind (primary circulation), and also the forward ground speed will be higher than that in the case of crabbing against the crosswind.

2. Materials and Methods

2.1. Aircraft Design and Capabilities

The UAV was codenamed Mystique VT and it has a wing span of 2.5 m and an overall length of 1.52 m, as shown in **Figure 1**. The relative control surface areas were deliberately kept small to avoid flutter and divergence at high speed. The MH 22 airfoil developed by Dr. Martin Hepperle for FAI pylon competition [19] was used on the main wing to help achieve high V_H. The power plant was a gasoline-powered Rossi 90 ducted engine (15 cc) with 315 mm tuned pipe. A 2-bladed variable pitch propeller was used to drive the aircraft to high cruising speed while providing sufficient static thrust for vertical hovering. The fuselage housed an 8 L capacity fuel tank system with distribution pumps to optimize the center of gravity required for cruising or spinsonde function. In general, the spinsonde maneuver required a more aft center of gravity. The fuel consumption rate of the engine at full throttle near sea-level was rated at 21 mL min^{-1} giving a total flight time of 6.3 hours at near

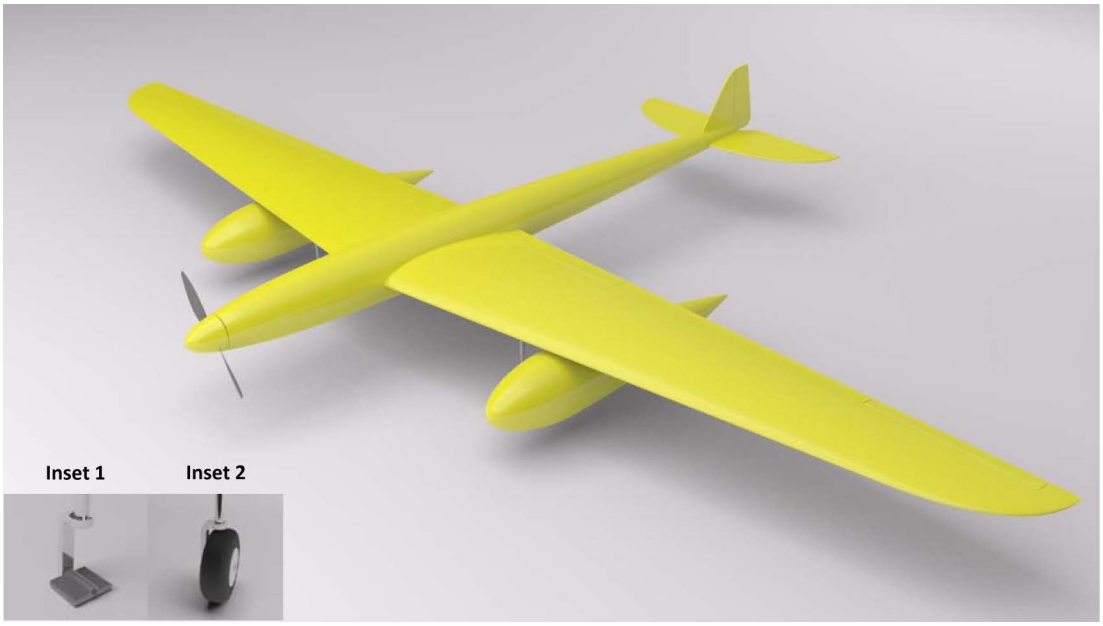

Figure 1. The Mystique VT with built-in spinsonde capability was designed for typhoon research. It has a wing span of 2.5 m and used the MH 22 airfoil. Fuel capacity of the optional drop tanks was 4 L each.

sea level. The aircraft was designed to have a thrust-to-weight ratio that exceeds unity when there is less than 3 L of fuel remaining in order to facilitate harrier maneuver or vertical descent during the final landing phase. This ability gives the aircraft the flexibility to operate with space-efficiency from land or carrier without the need for runway. Furthermore, optional drop tank of 4 L was added to each wing and the effects on the flight time and performance for land-based operation is evaluated. The wing loadings of the fully laden airplane with and without the drop tanks were 227 $g \cdot dm^{-2}$ and 140 $g \cdot dm^{-2}$, respectively.

The wing chord at root was 350 mm and each wing has an outer and inner aileron. Both the ailerons can be used for conventional roll function while the inner aileron was designed to give authoritative roll control during the harrier maneuver and vertical hovering as it is immersed in the propeller wash. The Mystique VT is equipped with a pair of retractable landing gears in tail dragger configuration. The base of the landing gear can be customized with magnetic plate system (Inset 1 in **Figure 1**) or wheel system (Inset 2 in **Figure 1**) depending on whether it is used for harrier docking or runway operation.

2.2. Simulation Details

The 3-dimensional model of the Mystique VT was created in Autodesk 3ds Max® software [20]. The orientations of the pivots and naming convention of the components were as per the requirements and the model was finally imported into the RealFlight®[1] 6.5 simulator [21] using the KEmax plugin [22]. Refinement of the physical model was done using the Accu-Model™ aircraft editor within the simulation software.

3. Simulation Results and Discussion

3.1. Steady Level Flight Performance

The Mystique VT was found to have stable and responsive level flights with good control over the roll, pitch and yaw. The maximum speeds in level flight with maximum continuous power (V_H) without and with the drop tanks were 355 ± 1 $km \cdot h^{-1}$ and 271 ± 1 $km \cdot h^{-1}$, respectively as shown in **Figure 2(a)** and **Figure 2(b)**.These results were obtained with maximum fuel load. Although the proposed approach of penetrating the storm was by "spiral entry" as proposed in the Introduction Section, it is interesting to note that the V_H of 355 $km \cdot h^{-1}$ is indeed higher than the sustained winds of the Category 5 Super Typhoon Haiyan of 315 $km \cdot h^{-1}$ [23]. Variation in V_H values with the propeller pitch for these two aircraft configurations were plotted in **Figure 3** along with the

[1]Real Flight is a registered trademark of Hobbico, Inc. used with permission.

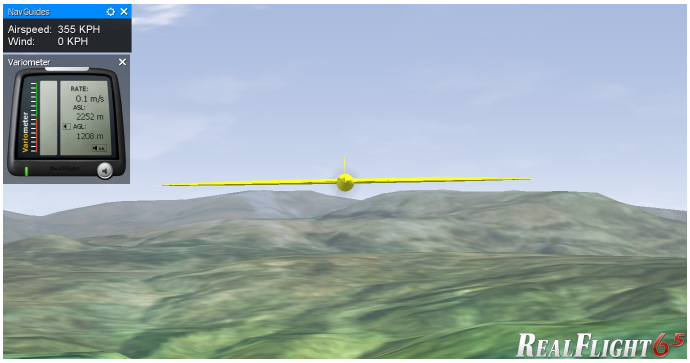

(a)

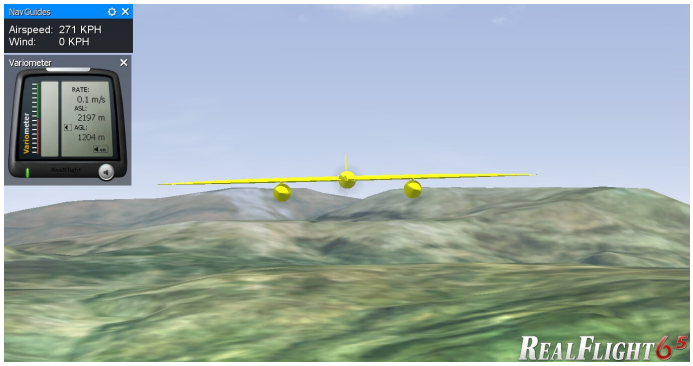

(b)

Figure 2. Level flight simulation tests revealed that the V_H of (a) Mystique VT was 355 km·h^{-1} while (b) that of the version with drop tanks was 271 km·h^{-1}.

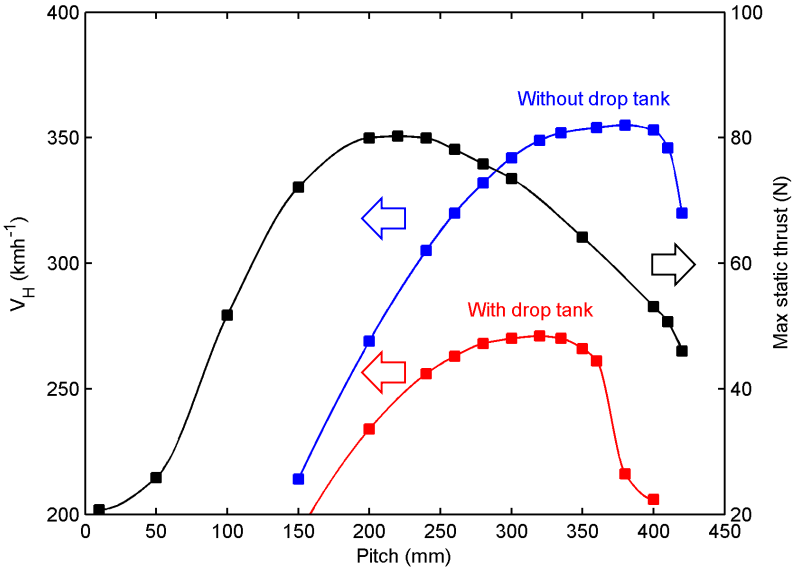

Figure 3. V_H values as a function of propeller pitch for the aircraft with and without the drop tanks. The corresponding static thrust was plotted on the secondary Y-axis on the right.

corresponding static thrusts on the secondary Y-axis (right side). A propeller pitch of 220 mm produced the maximum static thrust of 80.24 N. In general, a higher propeller pitch will result in a higher dynamic thrust but lower static thrust [24].

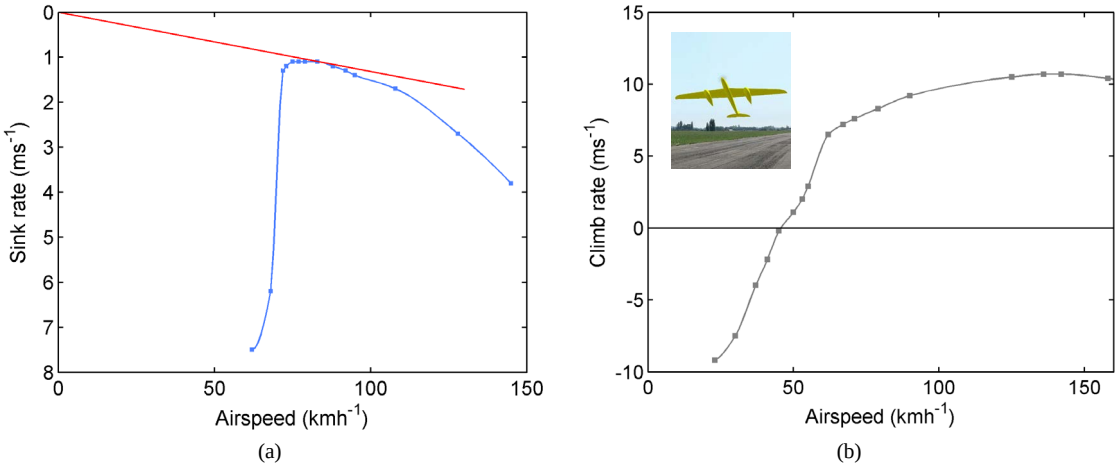

Figure 4. (a) Polar curve for the Mystique VT with drop tanks, and (b) steady-state climb rate at full throttle setting.

Gliding performance of the Mystique VT with drop tanks was characterized using the polar curve [**Figure 4(a)**]. The aircraft achieved a minimum sink rate of 1.1 ms^{-1} at an airspeed of about 80 $km \cdot h^{-1}$. The best L/D airspeed was 84 $km \cdot h^{-1}$ with a glide ratio of 21. The stall speed (V_{stall}) derived from the polar curve was 72 $km \cdot h^{-1}$. The plot in **Figure 4(b)** was obtained by repeating the same procedure to generate the polar curve, except this time with full throttle setting. It reveals that the horizontal airspeed as low as 46 $km \cdot h^{-1}$ was sufficient to keep the aircraft airborne at near sea-level. At such low speed and high nose angle, the aircraft is essentially performing the harrier maneuver. This feature would be particular useful, for example, as a method for the fully laden aircraft to safely execute a low-speed short landing without having to release the drop tanks. The inset in **Figure 4(b)** shows the fully loaded Mystique VT performing a full throttle harrier flyby.

Ground roll takeoff distance on an asphalt surface was evaluated for the Mystique VT with drop tanks as shown in **Figure 5**. The usual lift-off speed is $1.2V_{stall}$, however, given the climb rate of the aircraft presented in **Figure 4(b)**, we decided to abandon the general rule of thumb and set the takeoff safety speed (V_2) to be 74 $km \cdot h^{-1}$ and the required takeoff ground run distance was determined to be 58 m. Inset in **Figure 5** shows a demonstration in which the drop tanks were being released in midair.

3.2. High-Alpha Flight Performance

Figure 6 shows the Mystique VT in stationary vertical hover with 1 kg of fuel onboard. Given the fuel consumption of 21 $cm^3\ min^{-1}$ at full throttle, the remaining flight time was approximately 1 hour which would have provided more than sufficient safety of margin during the vertical landing phase. All the control surfaces were found to be authoritative during hovering. It could be observed in **Figure 6** that there was some deflection of the inner ailerons to counteract the propeller torque effect. The rate of response during hovering were found to be as follow—roll (right: 105˚ s^{-1}, left: 140˚ s^{-1}), pitch: 180˚ s^{-1} and yaw: 150˚ s^{-1}. It was harder to roll right because it was counteracting the propeller torque. Co-axial counter-rotating propellers similar to those recently being employed in the prestigious FAI World Championship for Aerobatic Model Aircraft (class F3A) could be used to eliminate the torque effect [25]. The maximum controlled vertical descent rate was found to be 3 ms^{-1}. Vertical takeoff was possible up to a maximum fuel load of 3 kg (4 L) with good control response. An 8 L fuel load (*i.e.*, fully laden without drop tanks) would require full throttle with static thrust of 80.24N, a launching angle of 45˚ to the vertical and a minimum horizontal takeoff speed of 22 $km \cdot h^{-1}$.

Figures 7(a)-(f) show the docking sequence for the Mystique VT. The landing sequence begun with the final approach and to be followed by a steep climb to reduce the forward airspeed. The motor thrust was gradually increased until the platform came to a transition hovering. The platform was then brought into a controlled vertical descent. The aircraft then made its way towards the docking surface using the harrier maneuver at a speed of about 15 $km \cdot h^{-1}$. The final speed prior to contact was typically less than 8 $km \cdot h^{-1}$. Being a typhoon UAV, it is essential that the Mystique VT has the ability to dock successfully under windy condition. Thus, simulation was set up to investigate its flight characteristics with strong crosswind docking. Results revealed that, apart

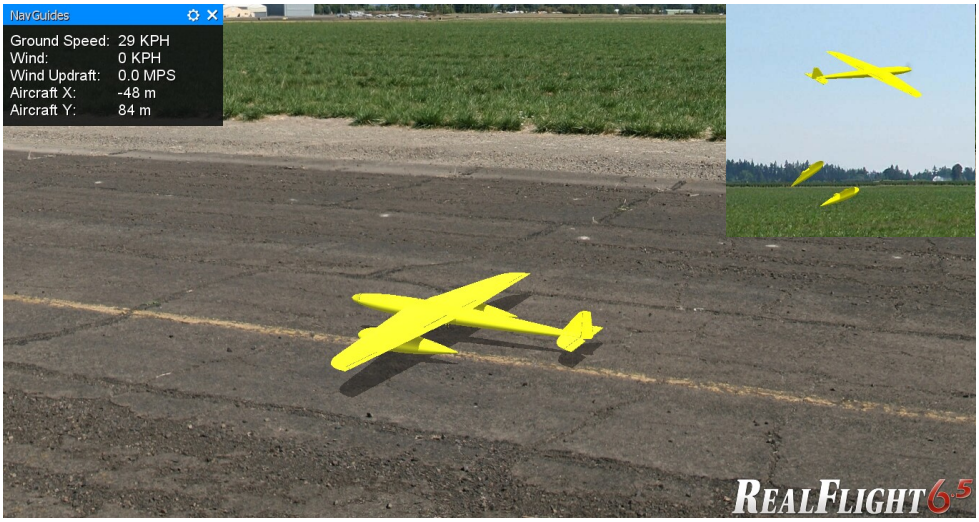

Figure 5. The fully laden Mystique VT equipped with drop tanks requires a takeoff distance of 58 m on an asphalt runway to reach V_2 of 74 km·h^{-1}. Inset: Demonstration of drop tanks being released.

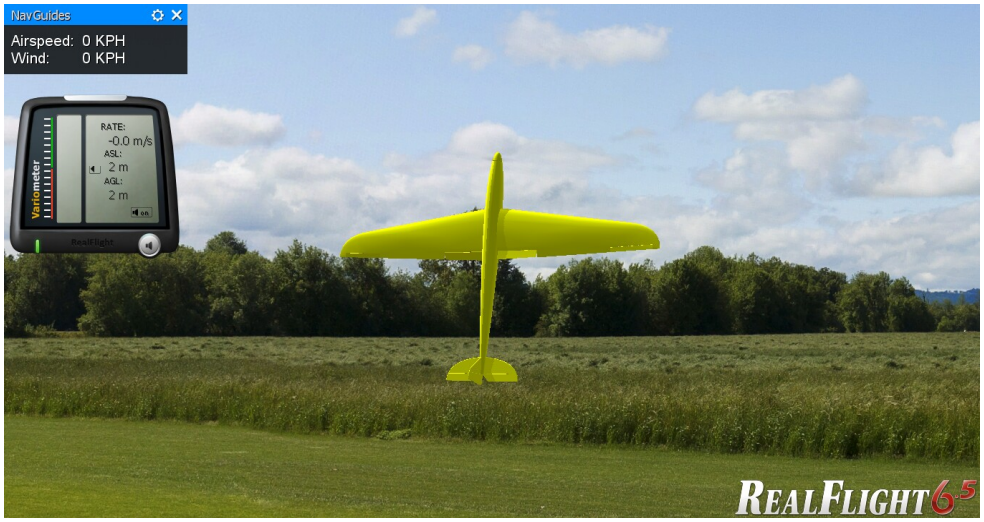

Figure 6. The Mystique VT in stationary hover. Slight deflection of the inner ailerons was necessary to counteract the propeller torque effect.

from a vertical crab angle (wind correction angle), the Mystique VT remained stable and controllable in crosswind of up to about 100 km·h^{-1} intensity as evidenced from **Figure 8**. Despite a wind speed of 102 km·h^{-1}, the aircraft was advancing at a ground speed of 2 km·h^{-1} with a descent rate of 0.2 ms^{-1}.

The high-alpha takeoff sequence was relatively straight-forward as depicted in **Figures 9(a)-(f)**. It begun with advancing the throttle to launch setting. Once the desired static thrust has been attained, the docking mechanism released the landing gears and the aircraft accelerated upward. Risk of wing-stall is almost non-existence in such configuration because the weight of the aircraft is primarily supported by the thrust of the propeller. In the final phase, the aircraft reduced its angle of attack and begun the steady state climb out.

3.3. Spinsonde

This section investigates how well the Mystique VT performs the spinsonde function which facilitates chute-free multi-cycle measurement of the vertical wind speed profiles of a tropical cyclone. The Mystique VT with and without the drop tanks would have their fuel load halved upon reaching their target measurement acquisition zones within the typhoon. The drop tanks would be almost empty by then and they will be released prior

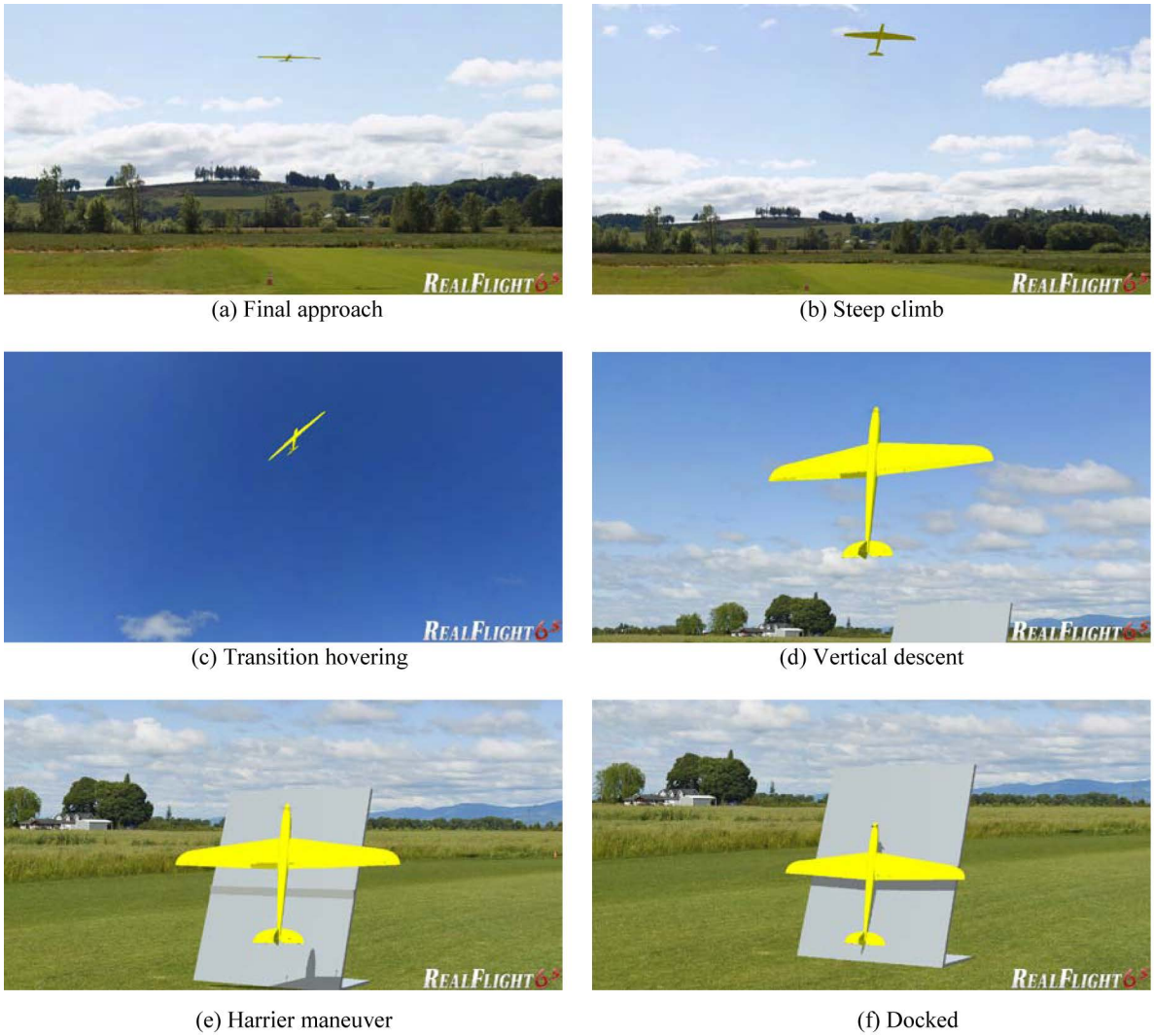

(a) Final approach (b) Steep climb

(c) Transition hovering (d) Vertical descent

(e) Harrier maneuver (f) Docked

Figure 7. The docking sequence.

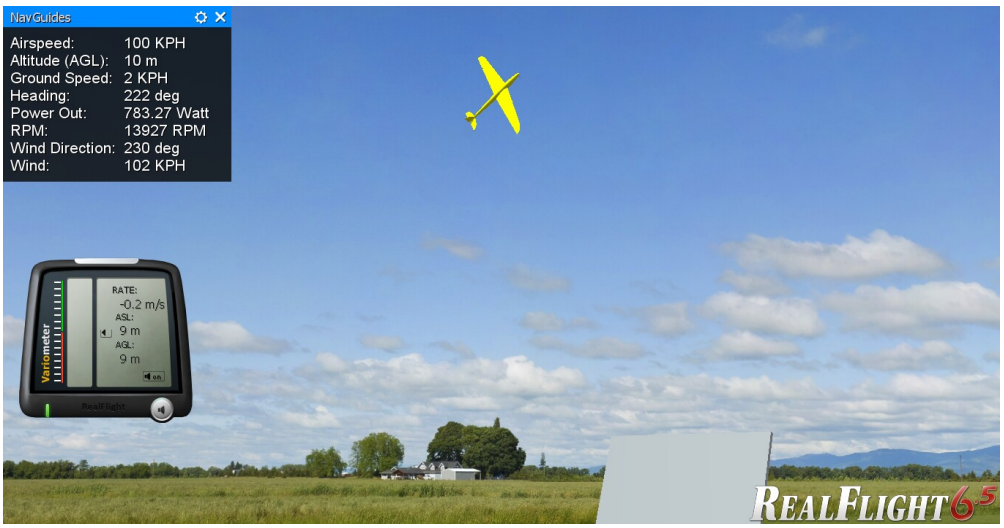

Figure 8. Simulated strong crosswind docking.

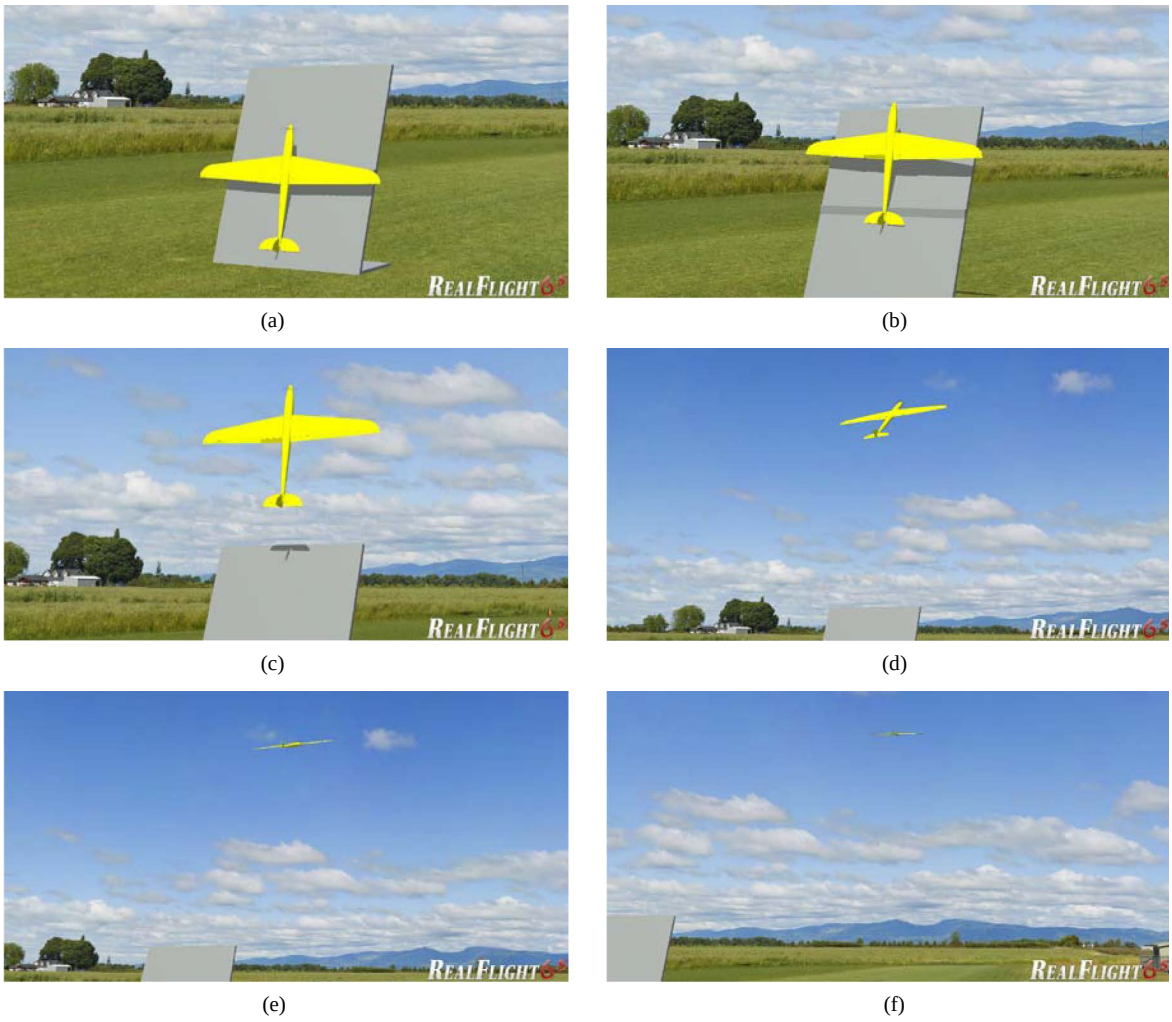

Figure 9. The high-alpha take-off sequence.

to performing the spinsonde. Thus, the fuel loads remaining for these two configurations of aircraft would be 8 L and 4 L, respectively. The aircraft were deliberately entered into a stall to initiate the maneuver. In general, the steady-state stall-spin was achieved by applying deflection of rudder and ailerons in the same direction and applying up elevator. The final angular displacements of all the three control surfaces were approximately 45˚. Wind speeds of 0 km·h^{-1} and over 200 km·h^{-1} were evaluated for both aircraft configurations.

Figure 10(a) and **Figure 10(b)** show the results for the aircraft with 4 L and 8 L fuel load, respectively in 0 km·h^{-1} wind with no drafts present. **Figure 10(c)** and **Figure 10(d)** show the spinsonde results in wind intensity of over 200 km·h^{-1} for both aircraft configurations. They performed the spinsonde function exceedingly well and it could be observed that the ground speeds were found to closely match the wind speeds to within ±3 km·h^{-1} in calm and strong wind scenarios. The stall-spin descent rates for the 4 L and 8 L configurations under no wind condition were 8.6 ± 0.1 and 9.8 ± 0.1 ms^{-1}, respectively which were slower than that of the chute-operated dropsonde of 11 ms^{-1}.This would translate to acquisition of higher resolution data. The 8 L configuration descended faster due to its higher wing loading. Note that the spinsonde tests in strong winds were carried out in a hilly environment with the presence of updrafts so the spinsonde descent rates were reduced for both aircraft configurations [**Figure 10(c)** and **Figure 10(d)**]. However, taking the magnitude of the updrafts into account, it could be observed that the true descent rates remained very much unaffected, e.g. 5.0 + 3.6 = 8.6 ms^{-1} for the 4 L case. Videos showing the stall-spin maneuvers including the exit to level flight in still air and strong winds are available as ancillary files (**1**, **2**, **3**, **4**). Additionally, it can be observed from the videos that the axis of rotation of the stall-spin is close to the center of gravity of the aircraft, similar to those reported by Poh (2015) [14], and

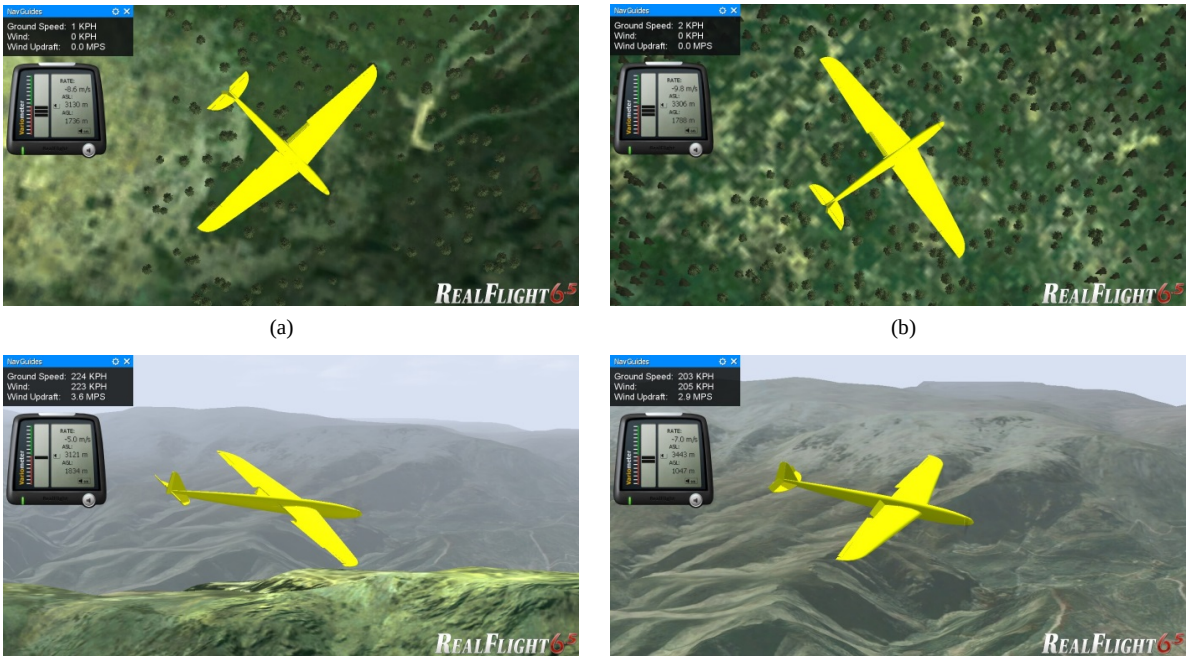

(a) (b)

(c) (d)

Figure 10. Evaluating the spinsonde performance: still air testing for (a) 4 L and (b) 8 L configurations; strong wind testing for (c) 4 L and (d) 8 L configurations. Note that the strong wind scenerios involved updrafts.

therefore the maneuver itself is not expected to affect the empirical GPS-based ground speed measurement as the sub-meter variation is significantly smaller than the resolution of GPS for civilian applications.

3.4. Flight Range and Viable Flight Schemes

To obtain an estimate of maximum flight range, the time spent performing the spinsonde will be neglected. A land-based Mystique VT will takeoff, fly into an approaching typhoon and return back to its base. It will spend half of the round trip with the drop tanks attached and thus its mean V_H is about 313 km·h^{-1} (average of 271 and 355 km·h^{-1}). On the other hands, the mean V_H of a Mystique VT not equipped with drop tanks was taken to be 355 km·h^{-1} throughout its entire journey. Consequently, the flight ranges of these two aircraft configurations were 3974 km and 2253 km, respectively. For a typhoon approaching land with forward speed of 20 km·h^{-1}, the Mystique VT with drop tanks will give a time-to-landfall window of 4.1 days in which to perform data analysis and to initiate hurricane evacuation, if necessary.

While the configuration without drop tanks gave a time-to-landfall of only 2.3 days, it was intended to offer operation versatility with its unique high-alpha launching and docking capabilities. It is ideal in applications where available space is at a premium such as on an aircraft carrier. A viable flight scheme would be to operate a fleet of Mystique VT's from a carrier within the eye of a tropical cyclone which is the calmest part of the storm with winds that usually do not exceed 24 km·h^{-1} [26]. Furthermore, the eye has a typical diameter of only 32 to 64 km [26] [27] which could be easily transversed by the aircraft given the total flight range of 2253 km. These aircraft will fly to systematically spaced locations in the eyewall region to acquire a set of vertical wind profiles using spinsonde technique.

A more elaborate design of the unmanned aircraft carrier involved a docking-launching system that would also provide stowage for the aircraft when not in operation so as to protect them from harsh elements such as gusty winds [28] (**Figure 11**). The underside of the docking surface could be populated with photovoltaic arrays for energy harvesting. This system offered the possibility for a fleet of Mystique VT's to operate autonomously in remote regions of the ocean for an extended period of time. The primary intended application was to study tropical cyclogenesis. Furthermore, it is interesting to note that cumulonimbus clouds over oceanic areas may not actually produce any significant thunder or lightning even in cloud towers with adequate instability and the reasons are still unclear [29]. Thus we hoped that the Mystique VT can also be used to investigate mesoscale

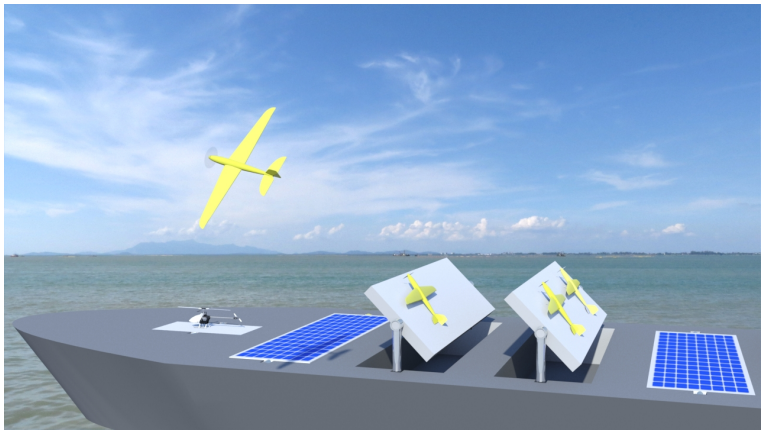

Figure 11. Rendition of a fleet of Mystique VT aircraft operating from an unmanned carrier with automatic stowage capability.

convective systems in the Intertropical Convergence Zone (ITCZ) as well as other related atmospheric research such as El Niño Southern Oscillation.

4. Conclusion

The design of an innovative tropical cyclone unmanned aerial vehicle codenamed Mystique VT had been proposed and its ability to fly into a typhoon and acquire the vertical wind speed profiles were evaluated via simulations. Results indicated that the aircraft has the following unique characteristics: 1) capable of vertical takeoff with maximum fuel load of 3 kg, 2) ability to perform harrier maneuver and vertical landing thereby offering the versatility to operate from land or aircraft carrier, 3) has excellent built-in spinsonde capability to acquire multiple vertical wind speed profiles in a single flight, and 4) V_H of 355 km·h^{-1} (271 km·h^{-1} when equipped with drop tanks). The UAV also has the potential to benefit related areas of research such as mesoscale convective systems in the Intertropical Convergence Zone.

References

[1] Dowdy, A.J., Qi, L., Jones, D., Ramsay, H., Fawcett, R. and Kuleshov, Y. (2012) Tropical Cyclone Climatology of the South Pacific Ocean and Its Relationship to El Niño—Southern Oscillation. *Journal of Climate*, **25**, 6108-6122. http://dx.doi.org/10.1175/JCLI-D-11-00647.1

[2] Cheung, K.K.W., Chang, L.T.C. and Li, Y. (2014) Rainfall Prediction for Landfalling Tropical Cyclones: Perspectives of Mitigation. Typhoon Impact and Crisis Management. *Advances in Natural and Technological Hazards Research*, **40**, 175-201. http://dx.doi.org/10.1007/978-3-642-40695-9_8

[3] Doocy, S., Dick, A., Daniels, A. and Kirsch, T.D. (2013) The Human Impact of Tropical Cyclones: A Historical Review of Events 1980-2009 and Systematic Literature Review. *PLOS Currents Disasters*.

[4] Chan, J.C.L. and Kepert, J.D. (2010) Global Perspectives on Tropical Cyclones: From Science to Mitigation. World Scientific Publishing Co. Pte Ltd., Singapore, 3-54. http://dx.doi.org/10.1142/7597

[5] NOAA (2013) Saffir-Simpson Hurricane Wind Scale. http://www.nhc.noaa.gov/aboutsshws.php

[6] Wikipedia (2015) Cyclogenesis. https://en.wikipedia.org/wiki/Cyclogenesis

[7] Hurricane Hunter Association (2015) Frequently Asked Questions. http://www.hurricanehunters.com/faq.htm

[8] Smith, R.K. (2006) Lectures on Tropical Cyclones. http://www.meteo.physik.uni-muenchen.de/lehre/roger/Tropical_Cyclones/060510_tropical_cyclones.pdf

[9] Franklin, J.L., Black, M.L. and Valde, K. (2003) GPS Drop Windsonde Wind Profiles in Hurricanes and Their Operational Implications. *Weather and Forecasting*, **18**, 32-44. http://dx.doi.org/10.1175/1520-0434(2003)018<0032:GDWPIH>2.0.CO;2

[10] Hille, K. (2014) Hurricane and Severe Storm Sentinel. National Aeronautics and Space Administration (NASA). http://www.nasa.gov/mission_pages/hurricanes/missions/hs3/overview/index.html#.Vidm2ewmym7

[11] Aerosonde Pty Ltd. (2015) Aerosonde® Unmanned Aircraft System (UAS).

http://www.aerosonde.com/products/products.html

[12] Hock, T. (2012) NCAR/NSF GV New Automated Dropsonde System Overview. National Center for Atmospheric Research Earth Observing Lab. http://www.eol.ucar.edu/projects/mpex/meetings/2012Dec/presentations/04_Hock.pdf

[13] Wikipedia (2013) Dropsonde. http://en.wikipedia.org/wiki/Dropsonde

[14] Poh, C.-K. and Poh, C.-H. (2015) Concept of Spinsonde for Multi-Cycle Measurement of Vertical Wind Profile of Tropical Cyclones. *Open Journal of Applied Sciences*, **5**, 145-150. http://dx.doi.org/10.4236/ojapps.2015.54015

[15] Selig, M.S. (2010) Modeling Full-Envelope Aerodynamics of Small UAVs in Realtime. *Proceedings of the AIAA Atmospheric Flight Mechanics Conference*, Ontario, 2-5 August 2010, AIAA 2010-7635. http://dx.doi.org/10.2514/6.2010-7635

[16] Academy of Model Aeronautics (2015) F5D. http://www.modelaircraft.org/files/f5d.pdf

[17] RC Media World (2014) World Record Attempt in Ballenstedt 2014. https://www.youtube.com/watch?v=1X6HEkyHNsQ

[18] Jorgensen, D.P., Zipser, E.J. and Lemone, M.A. (1985) Vertical Motions in Intense Hurricanes. *Journal of the Atmospheric Sciences*, **42**, 839-856. http://dx.doi.org/10.1175/1520-0469(1985)042<0839:VMIIH>2.0.CO;2

[19] Hepperle, M. (2004) MH 22. http://www.mh-aerotools.de/airfoils/mh22koo.htm

[20] Autodesk Inc. (2016) 3ds Max® 3D Modeling, Animation, and Rendering Software. http://www.autodesk.com/products/3ds-max/overview

[21] Great Planes® Model Mfg. (2015) RealFlight® Radio Control Flight Simulator. http://www.realflight.com/

[22] Knife Edge Software (2014) KEmax Content Creation Toolkit. http://www.knifeedge.com/KEmax/

[23] Mortillaro, N. (2013) Why Super Typhoon Haiyan Was So Destructive. http://globalnews.ca/news/955086/why-super-typhoon-haiyan-was-so-destructive/

[24] Hepperle, M. (2003) Static Thrust of Propellers. http://www.mh-aerotools.de/airfoils/prpstati.htm

[25] Ramel, M. (2013) Coaxial Drive Propulsion for F3A Models. http://www.sebart.it/img-F3A/coaxial-drive/coaxial-drive-description.html

[26] National Weather Service (2010) Tropical Cyclone Structure. National Oceanic and Atmospheric Administration (NOAA). http://www.srh.noaa.gov/jetstream/tropics/tc_structure.htm

[27] Piñeros, M.F., Ritchie, E.A. and Tyo, J.S. (2010) Detecting Tropical Cyclone Genesis from Remotely Sensed Infrared Image Data. *IEEE Geoscience and Remote Sensing Letters*, **7**, 826-830. http://dx.doi.org/10.1109/LGRS.2010.2048694

[28] Poh, C.-K. and Poh, C.-H. (2015) Intelligent Docking system with Automated Stowage for UAVs. Malaysia Patent Application No. PI 2015701399.

[29] Vasquez, T. (2009) The Intertropical Convergence Zone. Weatherwise. http://www.weatherwise.org/Archives/Back%20Issues/2009/Nov-Dec%202009/full-Intertropical-Converge.html